

Reservoir-Engineered Entanglement in Optomechanical Systems

Ying-Dan Wang and Aashish A. Clerk

Department of Physics, McGill University, 3600 rue University, Montreal, Quebec H3A 2T8, Canada
(Received 23 January 2013; published 18 June 2013)

We show how strong steady-state entanglement can be achieved in a three-mode optomechanical system (or other parametrically coupled bosonic system) by effectively laser cooling a delocalized Bogoliubov mode. This approach allows one to surpass the bound on the maximum stationary intracavity entanglement possible with a coherent two-mode squeezing interaction. In particular, we find that optimizing the relative ratio of optomechanical couplings, rather than simply increasing their magnitudes, is essential for achieving strong entanglement. Unlike typical dissipative entanglement schemes, our results cannot be described by treating the effects of the entangling reservoir via a Linblad master equation.

DOI: [10.1103/PhysRevLett.110.253601](https://doi.org/10.1103/PhysRevLett.110.253601)

PACS numbers: 42.50.Wk, 03.67.Bg, 42.50.Lc, 85.85.+j

Introduction.—The study of highly entangled quantum states is of interest both for fundamental reasons and for a myriad of applications in quantum information processing and quantum communication. Of particular fundamental interest is the possibility to entangle distinct macroscopic objects, a task made difficult by the unavoidable decoherence and dissipation associated with such systems. Equally interesting would be the ability to entangle photons of very different frequencies, e.g., microwave and optical photons.

A promising venue for the realization of both of these kinds of entanglement is provided by quantum optomechanics, where macroscopic mechanical degrees of freedom can be controlled, measured, and coupled using the modes of an electromagnetic cavity. Recent milestones in this field include the ability to cavity cool a mechanical resonator to its ground state of motion [1,2] and the observation of many-photon strong coupling effects [3–6]. A natural setting for entanglement generation is a three-mode optomechanical system consisting of two “target” modes to be entangled, which are each coupled to a third “auxiliary” mode. One could either have two optical target modes and a mechanical auxiliary mode, or vice versa; both variants have recently been achieved in experiment [7–9]. Several theoretical studies have described such schemes, using the basic idea that the auxiliary mode mediates an effective (coherent) two-mode squeezing interaction between the two target modes (see, e.g., Refs. [10–13]). However, such schemes typically yield at best a relatively small amount of intramode entanglement (something which we quantify more fully below).

In this Letter, we again consider generating steady-state entanglement of two bosonic modes in a three-mode system; while we focus on an optomechanical realization, our ideas could also be realized using superconducting circuits coupled via Josephson junctions [14,15] or other parametrically coupled three-bosonic-mode systems. Unlike previous works, we consider the possibility of entanglement via reservoir engineering [16]: we wish to tailor the dissipative environment of the two target modes such that the

dissipative dynamics relaxes the system into an entangled state. Such dissipative entanglement has been discussed in the context of atomic systems [17–21] and has even been realized experimentally [22].

The dissipative entanglement scheme we describe is related to optomechanical cavity-cooling schemes [23,24] which have been used successfully to cool mechanical resonators to the ground state. In our case, one is not cooling a simple mechanical mode to the ground state, but rather a hybrid mode delocalized over both target modes. In contrast to previous reservoir-engineering approaches to entanglement generation, where the dynamics is reduced to a simple Markovian master equation for the target degrees of freedom, our treatment is valid even in the regime where a simple adiabatic elimination of the intermediate mode is not possible. As we show, this regime turns out to be the most effective at generating entanglement. Our result shows that by optimizing the ratio of optomechanical coupling strengths, rather than simply increasing their magnitudes, this laser-cooling mechanism can be used to yield large amounts of time-independent intracavity entanglement. The amount of entanglement is far greater than in previous studies and, in fact, far greater than the maximum possible entanglement allowed by a coherent parametric interaction. Note that reservoir engineering in optomechanics has previously been studied theoretically, with the very different goal of generating long-range coherence in arrays [25].

System and normal modes.—While our scheme applies to a general bosonic three-mode system, we focus here on an optomechanical system where two optical or microwave cavity modes are coupled to a single mode of a mechanical resonator (see Fig. 1); see the Supplemental Material [26] for a discussion of entangling two mechanical modes coupled to a cavity mode. The Hamiltonian is

$$\hat{H} = \omega_M \hat{b}^\dagger \hat{b} + \sum_{i=1,2} (\omega_i \hat{a}_i^\dagger \hat{a}_i + g_i (\hat{b}^\dagger + \hat{b}) \hat{a}_i^\dagger \hat{a}_i) + \hat{H}_{\text{diss}}. \quad (1)$$

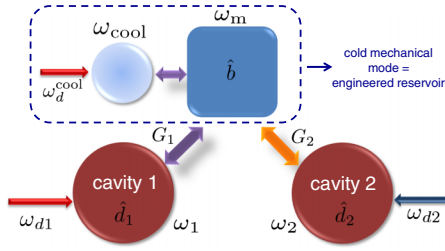


FIG. 1 (color online). Schematic of one realization of a three-mode optomechanical system, where two cavity modes are coupled to a single mode of a mechanical resonator. By driving cavity 1 (2) at the red (blue) detuned mechanical sideband, a dissipative entanglement mechanism is realized. To enhance the scheme, the mechanical resonator is cavity cooled and optically damped via a coupling to a third driven cavity mode, so that its total damping rate γ is greater than the damping rate κ of each cavity.

\hat{a}_i is the annihilation operator for cavity i (frequency ω_i , damping rate κ_i), \hat{b} is the annihilation operator of the mechanical mode (frequency ω_M , damping rate γ), and g_i are the optomechanical coupling strengths. \hat{H}_{diss} describes the dissipation of each mode, as well as the driving of the cavity modes. To achieve an entangling interaction, cavity 1 (2) is driven at the red (blue) sideband associated with the mechanical resonator: $\omega_{d1} = \omega_1 - \omega_M$ and $\omega_{d2} = \omega_2 + \omega_M$ [12]. We work in an interaction picture with respect to the cavity drives, and write $\hat{a}_i = \bar{a}_i + \hat{d}_i$ where \bar{a}_i is the classical cavity amplitude. We take $|\bar{a}_{1,2}| \gg 1$, which allows us to linearize the optomechanical interaction in the usual way (i.e., drop interaction terms not enhanced by the classical cavity amplitudes). The linearized Hamiltonian in the rotating frame is thus $\hat{H} = \omega_M(\hat{b}^\dagger \hat{b} + \hat{d}_1^\dagger \hat{d}_1 - \hat{d}_2^\dagger \hat{d}_2) + \hat{H}_{\text{int}} + \hat{H}_{\text{CR}} + \hat{H}_{\text{diss}}$ with

$$\hat{H}_{\text{int}} = G_1(\hat{b}^\dagger \hat{d}_1 + \hat{d}_1^\dagger \hat{b}) + G_2(\hat{b} \hat{d}_2 + \hat{d}_2^\dagger \hat{b}^\dagger), \quad (2)$$

$$\hat{H}_{\text{CR}} = G_1(\hat{b}^\dagger \hat{d}_1^\dagger + \hat{d}_1 \hat{b}) + G_2(\hat{b}^\dagger \hat{d}_2 + \hat{d}_2^\dagger \hat{b}). \quad (3)$$

Here $G_i = g_i \bar{a}_i$ (we take $g_i, \bar{a}_i > 0$ without loss of generality). We further focus on the resolved-sideband regime $\omega_M \gg \kappa_1, \kappa_2$, which suppresses the effects of the nonresonant interactions in \hat{H}_{CR} . The remaining interaction \hat{H}_{int} in Eq. (2) has the basic form suitable for entangling \hat{d}_1 and \hat{d}_2 : on a heuristic level, the parametric-amplifier interaction (G_2 term) first entangles \hat{d}_2 and \hat{b} , and then the beam-splitter interaction (G_1 term) swaps the \hat{b} and \hat{d}_1 states, thus yielding the desired entanglement.

Note that if one made the interactions in Eq. (2) nonresonant (e.g., by detuning the cavity drives from the sideband resonances by Δ), one could adiabatically eliminate the mechanical mode, resulting in a two-mode squeezing interaction $\hat{H}_{\text{TMS}} \simeq \lambda(\hat{d}_1 \hat{d}_2 + \text{H.c.})$ with $\lambda \sim G_1 G_2 / \Delta$ [27]. Such an interaction naturally leads to entanglement, but the amount is severely limited by the requirement of stability $\lambda \leq \kappa_{1,2}/2$. We quantify the entanglement using

the standard measure of the logarithmic negativity E_N (see the Supplemental Material [26]). One finds that the maximum stationary intracavity entanglement due to the two-mode squeezing coupling is (for $\kappa_1 = \kappa_2$ and zero temperature) $E_N = \ln(1 + 2\lambda/\kappa) \leq \ln 2 \sim 0.7$. Many suggested schemes for entanglement generation in optomechanical systems are limited by this stability requirement.

In contrast, the resonant case we consider allows for an alternative dissipative entanglement mechanism capable of much larger E_N . We will focus attention on the regime $G_2 < G_1$ where (for $\kappa_1 = \kappa_2$) our linear system is always stable (see the Supplemental Material [26]). Defining the effective two-mode squeezing parameter $r = \text{arctanh}(G_2/G_1)$, we introduce delocalized (canonical) cavity Bogoliubov mode operators:

$$\begin{aligned} \hat{\beta}_A &= \hat{d}_1 \cosh r + \hat{d}_2^\dagger \sinh r \equiv \hat{S}(r) \hat{d}_1 \hat{S}^\dagger(r), \\ \hat{\beta}_B &= \hat{d}_1^\dagger \sinh r + \hat{d}_2 \cosh r \equiv \hat{S}(r) \hat{d}_2 \hat{S}^\dagger(r). \end{aligned} \quad (4)$$

Here, $\hat{S}(r) \equiv \exp[r \hat{d}_1 \hat{d}_2 - \text{H.c.}]$ is a two-mode squeezing operator. It thus follows that the joint vacuum of $\hat{\beta}_A, \hat{\beta}_B$ is the two-mode squeezed state $|r\rangle = \hat{S}(r)|0, 0\rangle$, where $|0, 0\rangle$ is the vacuum of \hat{d}_1, \hat{d}_2 . The entanglement of this state is simply $E_N = 2r$.

In terms of these new operators, $\hat{H}_0 = \omega_M(\hat{b}^\dagger \hat{b} + \hat{\beta}_A^\dagger \hat{\beta}_A - \hat{\beta}_B^\dagger \hat{\beta}_B)$ and the optomechanical interactions in Eqs. (2) and (3) take the simple form

$$\hat{H}_{\text{int}} = \tilde{G} \hat{\beta}_A^\dagger \hat{b} + \text{H.c.}, \quad \hat{H}_{\text{CR}} = \tilde{G} \hat{\beta}_A^\dagger \hat{b}^\dagger + \text{H.c.}, \quad (5)$$

where $\tilde{G} \equiv \sqrt{G_1^2 - G_2^2}$. The mode $\hat{\beta}_B$ completely decouples from the mechanics (it is a mechanically dark mode [28,29]), while in the good-cavity limit of interest \hat{H}_{CR} can be neglected, implying that the mode $\hat{\beta}_A$ has a simple beam-splitter interaction with the mechanics. $\hat{H}_0 + \hat{H}_{\text{int}}$ is trivially diagonalized, resulting in hybridized modes $\hat{\beta}_\pm = (\hat{\beta}_A \pm \hat{b})/\sqrt{2}$ with energies $\omega_M \pm \tilde{G}$. The existence of three distinct eigenmodes (two hybrid, one dark) can be useful to understand entanglement (in particular spectral entanglement [13,30]) in the case where the mechanical mode is driven by excessive thermal noise; we will discuss this in a future work. We focus here on generating intracavity entanglement, which has the benefit of being insensitive to whether internal losses contribute to the damping rate κ of the cavities.

We now exploit the fact that Eq. (5) has exactly the form used for standard cavity cooling [23,24]. Thus, if we can couple the mechanical mode \hat{b} to a cold reservoir, then the beam-splitter coupling \hat{H}_{int} can be used to cool $\hat{\beta}_A$ towards vacuum, resulting in a stationary entangled state. A high-frequency, low-Q mechanical resonator would thus be ideal. Alternatively, we will take the mechanical mode to be coupled to a third cavity mode which is used to laser cool its thermal occupancy towards the ground state by providing a source of cold damping (see Fig. 1). In what

follows, we include the cooling cavity coupled to the mechanical resonator in the definition of its effective thermal bath; hence, the damping rate γ includes the large contribution of the optical damping. Amusingly, our scheme is one of the few examples in optomechanics where the enhanced mechanical damping rate resulting from cavity cooling is actually highly beneficial.

Langevin equations and cavity cooling.—To describe the cooling potential of \hat{H}_{int} , we next use input-output theory to derive the Heisenberg-Langevin equations for our linearized system. These take the standard form

$$\begin{aligned} \frac{d}{dt} \hat{b} &= \left(-i\omega_M - \frac{\gamma}{2}\right) \hat{b} - i(G_1 \hat{d}_1 + G_2 \hat{d}_2^\dagger) - \sqrt{\gamma} \hat{b}_{\text{in}}, \\ \frac{d}{dt} \hat{d}_1 &= \left(-i\omega_M - \frac{\kappa_1}{2}\right) \hat{d}_1 - iG_1 \hat{b} - \sqrt{\kappa_1} \hat{d}_{1,\text{in}}, \\ \frac{d}{dt} \hat{d}_2^\dagger &= \left(-i\omega_M - \frac{\kappa_2}{2}\right) \hat{d}_2^\dagger + iG_2 \hat{b} - \sqrt{\kappa_2} \hat{d}_{2,\text{in}}, \end{aligned} \quad (6)$$

where $\hat{d}_{i,\text{in}}$, \hat{b}_{in} describes operator-valued white noise driving the cavity and mechanical modes, and we have taken the good-cavity limit $\omega_M \gg \kappa$ (allowing us to drop terms due to \hat{H}_{CR}). Equations (6) are readily solved to find the steady-state occupancy and correlation of the Bogoliubov modes. In the following analytic expressions, we take $\kappa_1 = \kappa_2$ for simplicity and focus on the good-cavity limit (though Fig. 2 includes corrections due to \hat{H}_{CR}).

Imagine first that the optomechanical interactions vanished, i.e., $\hat{H}_{\text{int}} = 0$, and consider the behavior of $\hat{\beta}_A$, $\hat{\beta}_B$ (defined for a fixed $r > 0$). Even at zero temperature, $\hat{\beta}_A$ and $\hat{\beta}_B$ will have a nonzero occupancy: the Bogoliubov transformation of Eq. (4) implies that vacuum noise driving the cavities acts as effective thermal noise for $\hat{\beta}_A$, $\hat{\beta}_B$. Writing these intrinsic ($\hat{H}_{\text{int}} = 0$) occupancies as $\langle \hat{\beta}_j^\dagger \hat{\beta}_j \rangle_0 = \bar{n}_{\text{th},j}$ we have

$$\bar{n}_{\text{th},A/B} = \bar{n}_{\text{th},1/2} \cosh^2 r + (\bar{n}_{\text{th},2/1} + 1) \sinh^2 r. \quad (7)$$

Here, $\bar{n}_{\text{th},1}$ ($\bar{n}_{\text{th},2}$) represents the temperature of the thermal bath coupled to cavity 1 (2). As one increases the squeeze parameter r , the effective heating of the $\hat{\beta}_j$ modes becomes exponentially large, implying the state of the system is far from being an ideal two-mode squeezed vacuum state; the state is not entangled.

Including now the effects of H_{int} [and taking $r = \text{arctanh}(G_2/G_1)$], the dark-mode $\hat{\beta}_B$ is unaffected, whereas the occupancy of $\hat{\beta}_A$ is modified to

$$\begin{aligned} \langle \hat{\beta}_A^\dagger \hat{\beta}_A \rangle &= \frac{\kappa}{\Gamma_{\text{opt}} + \kappa} \left(1 + \frac{\Gamma_{\text{opt}}}{\gamma + \kappa}\right) \bar{n}_{\text{th},A} \\ &+ \frac{\Gamma_{\text{opt}} \gamma}{(\Gamma_{\text{opt}} + \kappa)(\gamma + \kappa)} \bar{n}_{\text{th},M}, \end{aligned} \quad (8)$$

where $\bar{n}_{\text{th},M}$ represents the temperature of the mechanical bath (which includes the cooling cavity), and the effective ‘‘cold damping rate’’ of $\hat{\beta}_A$ by the mechanics is

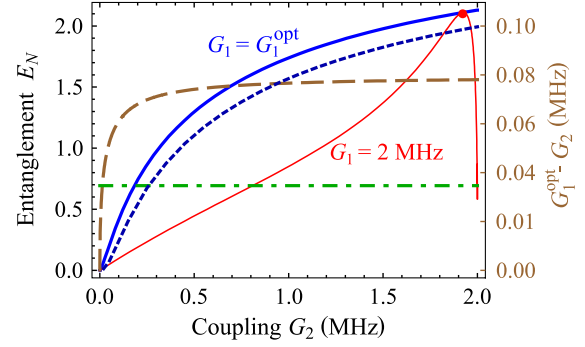


FIG. 2 (color online). Stationary intracavity entanglement (as quantified by log negativity E_N , left scale) as a function of the entangling interaction G_2 . We take $\bar{n}_{\text{th},1} = \bar{n}_{\text{th},2} = 0$, a mechanical frequency of $\omega_M = 2\pi \times 10$ MHz, damping $\gamma = 2\pi \times 0.8$ MHz, and do not make the rotating wave approximation. The solid red thin curve corresponds to a fixed value of $G_1 = 2\pi \times 2$ MHz, and $\kappa_1 = \kappa_2 = 2\pi \times 50$ kHz. One clearly sees a nonmonotonic dependence on G_2 . The solid blue thick curve and short-dashed blue curve instead correspond to tuning G_1 to the value G_1^{opt} for each G_2 , such that the dissipative entangling mechanism can be optimized. The value of $G_1^{\text{opt}} - G_2$ [cf. Eq. (10)] is indicated by the long-dashed brown curve (right scale). The solid blue (dashed blue) curve corresponds to $\kappa_1 = \kappa_2 = 50$ kHz ($\kappa_{1/2}/2\pi = 45$ kHz, 55 kHz) and $\bar{n}_{\text{th},M} = 0$ ($\bar{n}_{\text{th},M} = 0.3$). The green dash-dotted line represents the maximum stationary entanglement achievable with a coherent two-mode squeezing interaction $E_N = \ln 2$.

$\Gamma_{\text{opt}} \equiv 4\tilde{G}^2/\gamma$. This is the familiar equation for cavity cooling in the good-cavity limit, where now the mechanics plays the role of a cold reservoir. For $\bar{n}_{\text{th},M} = 0$ and weak coupling ($\Gamma_{\text{opt}} \ll \gamma$), the $\hat{\beta}_A$ mode is cooled by a factor $\kappa/(\kappa + \Gamma_{\text{opt}})$. In the strong coupling limit, the cooling factor saturates to a value $\kappa/(\gamma + \kappa)$.

Thus, while even vacuum noise tends to heat $\hat{\beta}_A$, $\hat{\beta}_B$ to an exponentially large effective temperature, the optomechanical interaction of Eq. (5) can be used to cool $\hat{\beta}_A$. Using the inequality of Duan *et al.* [31], one can show that if one cools $\hat{\beta}_A$ so that

$$\langle \hat{\beta}_A^\dagger \hat{\beta}_A \rangle \leq \sinh^2 r, \quad (9)$$

then the two cavities must necessarily be entangled (see the Supplemental Material [26]). As the orthogonal Bogoliubov mode $\hat{\beta}_B$ is decoupled from the mechanics, it is not cooled, making it impossible to achieve an ideal two-mode squeezed vacuum state. Nonetheless, we find that simply cooling $\hat{\beta}_A$ is sufficient to generate a steady state with significant entanglement ($E_N \sim 2r - \ln 2$ in the large r limit); this is despite the fact that the resulting state has negligible overlap with a two-mode squeezed vacuum (see the Supplemental Material [26]).

To rigorously quantify the cavity-cavity entanglement, we compute and discuss in what follows the log negativity

E_N , which is a function of the covariance matrix; details are provided in the Supplemental Material [26].

Maximizing entanglement.—We now see that entanglement generation is more subtle than one might expect given the simple form of Eq. (2). In particular, if G_1 is fixed, the amount of stationary entanglement is a nonmonotonic function of the entangling-interaction strength G_2 (see Fig. 2). The dissipative entanglement mechanism discussed here directly explains this behavior, as increasing G_2 has two opposing effects: it not only increases r and the delocalization of the Bogoliubov modes (enhancing entanglement), but also increases the effective temperature of these modes. This latter effect is due both to an increase in the effective temperature of the cavity vacuum noise [cf. Eq. (7)], and to a suppression of the cavity-cooling effect (as the effective coupling \tilde{G} decreases with increasing G_2).

The maximum entanglement is achieved by carefully balancing the opposing tendencies described above; without this optimization, the entanglement will remain small. For fixed couplings G_1, G_2 , one can optimize the entanglement as a function of the mechanical damping γ . The maximum occurs at a nonzero dissipation strength, which at zero mechanical temperature and in the good-cavity limit is simply given by $\gamma = 2\tilde{G}$. This value simply minimizes the occupancy of $\hat{\beta}_A$, and corresponds to a simple impedance matching condition (i.e., the rate with which the $\hat{\beta}_A$ mode and mechanics exchange energy matches the rate at which the mechanics and its bath exchange energy).

More relevant to experiment is to consider κ and γ fixed, and optimize the entanglement over coupling strength. Focusing on the most interesting regime where the cooperativity $C_2 \equiv G_2^2/(\gamma\kappa) \gg 1$, and considering the good-cavity limit and zero temperature (the mechanical resonator is also cooled to vacuum by the third cavity mode), we find that for fixed G_2 , the optimal G_1 is given by

$$G_1^{\text{opt}} \approx G_2 + \sqrt{\frac{\kappa\gamma}{8}} \left(1 + \frac{2\kappa}{\gamma}\right), \quad \text{i.e., } \frac{\tilde{G}^{\text{opt}}}{\gamma} \approx \left(\frac{C_2\kappa^2}{2\gamma^2}\right)^{1/4}. \quad (10)$$

Note that for large C_2 , this optimal value can easily correspond to a strong interaction $\tilde{G} > \kappa, \gamma$. Thus, in this optimal regime, the effects of our “engineered reservoir” (cold mechanical resonator) on the target cavity modes cannot be described by a Markovian dissipator in a master equation; this is in stark contrast to standard dissipation-by-entanglement schemes.

For the optimal value of G_1 above, the entanglement takes simple forms in two relevant limits. If we hold C_2 fixed while taking the limit $\gamma/\kappa \rightarrow \infty$, we have (at zero temperature)

$$E_N^{\text{opt}} \approx \frac{1}{2} \ln[2C_2] = 2r - 2\ln 2. \quad (11)$$

For large C_2 , the entanglement is almost that of a two-mode squeezed vacuum (i.e., $E_N = 2r$). Alternatively, we could hold the ratio γ/κ fixed and let $C_2 \rightarrow \infty$; we have (at zero temperature)

$$E_N^{\text{opt}} \sim \ln\left(2 + \frac{\gamma}{\kappa} + \mathcal{O}\left[\frac{(\gamma/\kappa)^2}{\sqrt{C_2}}\right]\right). \quad (12)$$

This is the strong-interaction limit, where the $\hat{\beta}_A$ mode hybridizes with the mechanical resonator. The maximal cooling of $\hat{\beta}_A$ is consequently set by the ratio γ/κ [cf. Eq. (8)]. The amount of entanglement here increases monotonically from $\ln 2$ (the maximum possible with a coherent coupling) as this cooling factor is increased.

The behavior of the stationary entanglement versus coupling strength is shown in Fig. 2, where we have used parameters similar to those achieved in recent state-of-the-art experiments on microwave-circuit optomechanical systems [1,5]. We assume that a $\omega_M = 10$ MHz mechanical resonator is first cavity cooled to near its ground state, with a final damping rate of $\gamma = 0.8$ MHz (which is predominantly due to the cold optical damping used for the cooling). By then optimally tuning the couplings to the target modes G_1, G_2 to optimize the dissipative entanglement mechanism (while keeping them $\lesssim 2.2$ MHz), one can obtain a relatively large $E_N \sim 2.1$. This exceeds by an order-of-magnitude the intracavity entanglement obtained in previous studies of the same system [12], as well as the maximum of $\ln 2$ possible with a coherent two-mode squeezing interaction. If this entanglement was used for a teleportation experiment, the maximum possible fidelity would be 0.89 [32,33]; this reduces the error by a factor of 3 compared to what would be possible with $E_N = \ln 2$. Figure 2 also shows that

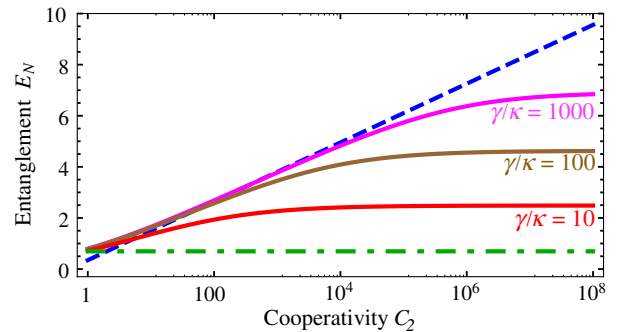


FIG. 3 (color online). Intracavity stationary entanglement (quantified by E_N) versus cooperativity C_2 , where we use an optimized choice for G_1 [as given by Eq. (10)], and have taken $\kappa_1 = \kappa_2$ and zero temperature. The solid lines correspond to different choices of the damping ratio γ/κ as indicated; increasing γ/κ increases the amount that one can cool the delocalized $\hat{\beta}_A$ mode, and hence enhances entanglement. For large C_2 , these curves asymptote to the value in Eq. (12). The dashed blue line is the asymptotic expression of Eq. (11). The green dashed-dotted line indicates $E_N = \ln 2$ (the maximum E_N possible with a two-mode squeezing interaction).

large values of E_N are possible even when $\bar{n}_{\text{th},M} \neq 0$ and $\kappa_1 \neq \kappa_2$.

In Fig. 3 we show how the stationary entanglement grows to dramatically large values with C_2 for an optimized choice of G_1 . While the parameters needed for such E_N may be out of reach in current-generation optomechanics experiments, they may be more feasible by implementing a superconducting circuit realization of our scheme [14,15].

Conclusions.—We have presented a general method for the dissipative generation of entanglement in a three-mode optomechanical system. The entanglement generated here could be verified by measuring the covariance matrix of the two target cavity modes using homodyne techniques (see, e.g., Ref. [11]). Alternatively, one could directly use the cavity output spectra at resonance to measure the occupancy of the $\hat{\beta}_A$ mode; verifying that it violates the Duan inequality of Eq. (9) would also confirm the generation of entanglement (see the Supplemental Material [26]).

We thank S. Chesi and L. Tian for useful conversations. This work was supported by the DARPA ORCHID program under a grant from the AFOSR.

-
- [1] J. D. Teufel, T. Donner, D. Li, J. W. Harlow, M. S. Allman, K. Cicak, A. J. Sirois, J. D. Whittaker, K. W. Lehnert, and R. W. Simmonds, *Nature (London)* **475**, 359 (2011).
- [2] J. Chan, T. P. M. Alegre, A. H. Safavi-Naeini, J. T. Hill, A. Krause, S. Gröblacher, M. Aspelmeyer, and O. Painter, *Nature (London)* **478**, 89 (2011).
- [3] S. Weis, R. Riviere, S. Deleglise, E. Gavartin, O. Arcizet, A. Schliesser, and T. Kippenberg, *Science* **330**, 1520 (2010).
- [4] A. H. Safavi-Naeini, T. P. M. Alegre, J. Chan, M. Eichenfield, M. Winger, Q. Lin, J. T. Hill, D. E. Chang, and O. Painter, *Nature (London)* **472**, 69 (2011).
- [5] J. D. Teufel, D. Li, M. S. Allman, K. Cicak, A. J. Sirois, J. D. Whittaker, and R. W. Simmonds, *Nature (London)* **471**, 204 (2011).
- [6] E. Verhagen, S. Deleglise, S. Weis, A. Schliesser, and T. Kippenberg, *Nature (London)* **482**, 63 (2012).
- [7] J. T. Hill, A. H. Safavi-Naeini, J. Chan, and O. Painter, *Nat. Commun.* **3**, 1196 (2012).
- [8] C. Dong, V. Fiore, M. C. Kuzyk, and H. Wang, *Science* **338**, 1609 (2012).
- [9] F. Massel, S. U. Cho, J.-M. Pirkkalainen, P. Hakonen, T. T. Heikkilä, and M. A. Sillanpää, *Nat. Commun.* **3**, 987 (2012).
- [10] S. Mancini, V. Giovannetti, D. Vitali, and P. Tombesi, *Phys. Rev. Lett.* **88**, 120401 (2002).
- [11] M. Paternostro, D. Vitali, S. Gigan, M. S. Kim, C. Brukner, J. Eisert, and M. Aspelmeyer, *Phys. Rev. Lett.* **99**, 250401 (2007).
- [12] S. Barzanjeh, D. Vitali, P. Tombesi, and G. J. Milburn, *Phys. Rev. A* **84**, 042342 (2011).
- [13] S. Barzanjeh, M. Abdi, G. J. Milburn, P. Tombesi, and D. Vitali, *Phys. Rev. Lett.* **109**, 130503 (2012).
- [14] N. Bergeal, R. Vijay, V. E. Manucharyan, I. Siddiqi, R. J. Schoelkopf, S. M. Girvin, and M. Devoret, *Nat. Phys.* **6**, 296 (2010).
- [15] B. Peropadre, D. Zueco, F. Wulchner, F. Deppe, A. Marx, R. Gross, and J. J. Garcia-Ripoll, *Phys. Rev. B* **87**, 134504 (2013).
- [16] J. F. Poyatos, J. I. Cirac, and P. Zoller, *Phys. Rev. Lett.* **77**, 4728 (1996).
- [17] M. B. Plenio and S. F. Huelga, *Phys. Rev. Lett.* **88**, 197901 (2002).
- [18] B. Kraus and J. I. Cirac, *Phys. Rev. Lett.* **92**, 013602 (2004).
- [19] A. S. Parkins, E. Solano, and J. I. Cirac, *Phys. Rev. Lett.* **96**, 053602 (2006).
- [20] B. Kraus, H. P. Büchler, S. Diehl, A. Kantian, A. Micheli, and P. Zoller, *Phys. Rev. A* **78**, 042307 (2008).
- [21] H. Krauter, C. A. Muschik, K. Jensen, W. Wasilewski, J. M. Petersen, J. I. Cirac, and E. S. Polzik, *Phys. Rev. Lett.* **107**, 080503 (2011).
- [22] C. A. Muschik, E. S. Polzik, and J. I. Cirac, *Phys. Rev. A* **83**, 052312 (2011).
- [23] F. Marquardt, J. P. Chen, A. A. Clerk, and S. M. Girvin, *Phys. Rev. Lett.* **99**, 093902 (2007).
- [24] I. Wilson-Rae, N. Nooshi, W. Zwerger, and T. J. Kippenberg, *Phys. Rev. Lett.* **99**, 093901 (2007).
- [25] A. Tomadin, S. Diehl, M. D. Lukin, P. Rabl, and P. Zoller, *Phys. Rev. A* **86**, 033821 (2012).
- [26] See Supplemental Material at <http://link.aps.org/supplemental/10.1103/PhysRevLett.110.253601> for details on the calculation, a discussion of the two mechanical resonator system, and details on the cavity output spectrum.
- [27] M. Schmidt, M. Ludwig, and F. Marquardt, *New J. Phys.* **14**, 125005 (2012).
- [28] Y.-D. Wang and A. A. Clerk, *Phys. Rev. Lett.* **108**, 153603 (2012).
- [29] L. Tian, *Phys. Rev. Lett.* **108**, 153604 (2012).
- [30] C. Wipf, T. Corbitt, Y. Chen, and N. Mavalvala, *New J. Phys.* **10**, 095017 (2008).
- [31] L.-M. Duan, G. Giedke, J. I. Cirac, and P. Zoller, *Phys. Rev. Lett.* **84**, 2722 (2000).
- [32] G. Adesso and F. Illuminati, *Phys. Rev. Lett.* **95**, 150503 (2005).
- [33] A. Mari and D. Vitali, *Phys. Rev. A* **78**, 062340 (2008).